

Final Report

**IMPLEMENTING PM CHEMISTRY
IN THE CAMx “IRON PiG”
PLUME-IN-GRID MODULE**

Prepared for

Lake Michigan Air Directors Consortium
2250 E. Devon Avenue
Des Plaines, IL 60018

Prepared by

Chris Emery
Greg Yarwood

ENVIRON International Corporation
101 Rowland Way, Suite 220
Novato, CA 94945

March 2005

ACKNOWLEDGEMENTS

The authors wish to acknowledge the contributions made by Dr. Paul Guthrie and Dr. Mark Yocke toward the development of the IRON PiG model. Both contributed significantly to the initial concepts, design, and implementation of full chemistry into the PiG framework. Dr. Guthrie developed the initial IRON PiG source code. Dr. Yocke guided the development of ancillary PiG components, such as the addition of the RTRAC Probing Tool into the PiG framework, and puff sampling.

TABLE OF CONTENTS

	Page
1. INTRODUCTION.....	1-1
1.1 Background.....	1-1
2. THE CAMx IRON PiG	2-1
2.1 Basic Puff Structure and Diffusive Growth.....	2-1
2.2 Puff Transport.....	2-4
2.3 Modifications Specific to IRON PiG.....	2-5
3. IMPLEMENTING PM CHEMISTRY AND DEPOSITION INTO IRON PiG.....	3-1
3.1 PM Chemistry.....	3-1
3.2 Dry and Wet Deposition.....	3-2
4. PRELIMINARY IRON PiG TESTING AND EVALUATION.....	4-1
4.1 Setup.....	4-1
4.2 Evaluation.....	4-2
4.3 Guidance on Testing PM PiG.....	4-2
4.4 Recommendations.....	4-15
REFERENCES.....	R-1

TABLES

Table 4-1. Configuration of the preliminary PM PiG test case.....	4-1
---	-----

FIGURES

Figure 4-1. Ozone concentrations (ppm) in layer 1 for the PM PiG run (top) and for the difference between the PM PiG and no-PiG runs (bottom).	4-3
Figure 4-2. Ozone concentrations (ppm) in layer 5 for the PM PiG run (top) and for the difference between the PM PiG and no-PiG runs (bottom).	4-4
Figure 4-3. SO ₂ concentrations (ppm) in layer 5 for the PM PiG run (top) and for the difference between the PM PiG and no-PiG runs (bottom).	4-5
Figure 4-4. Sulfate concentrations (µg/m ³) in layer 5 for the PM PiG run (top) and for the difference between the PM PiG and no-PiG runs (bottom).	4-6

Figure 4-5. Nitrate concentrations ($\mu\text{g}/\text{m}^3$) in layer 5 for the PM PiG run (top) and for the difference between the PM PiG and no-PiG runs (bottom). 4-7

Figure 4-6. Ammonium concentrations ($\mu\text{g}/\text{m}^3$) in layer 5 for the PM PiG run (top) and for the difference between the PM PiG and no-PiG runs (bottom). 4-8

Figure 4-7. Total secondary inorganic PM concentrations ($\mu\text{g}/\text{m}^3$) in layer 5 for the PM PiG run (top) and for the difference between the PM PiG and no-PiG runs (bottom). 4-9

Figure 4-8. Secondary organic aerosol concentrations ($\mu\text{g}/\text{m}^3$) in layer 5 for the PM PiG run (top) and for the difference between the PM PiG and no-PiG runs (bottom). 4-10

Figure 4-9. SO_2 dry deposited mass (g/ha) for the PM PiG run (top) and for the difference between the PM PiG and no-PiG runs (bottom). 4-11

Figure 4-10. SO_2 wet deposited mass (g/ha) for the PM PiG run (top) and for the difference between the PM PiG and no-PiG runs (bottom). 4-12

1. INTRODUCTION

Under the sponsorship of the Lake Michigan Air Directors Consortium (LADCO), ENVIRON is improving the PM modeling capabilities in CAMx version 4, including adding Particulate Source Apportionment Technology (PSAT), improving the wet deposition algorithm, updating the Carbon Bond IV (CB4) gas-phase chemical mechanism, and adding PM to the new full-chemistry version of the Plume-in-Grid (PiG) module. At a LADCO/MRPO modeling workshop in March 2003, several groups expressed interest in extending the CAMx PiG model to include PM. We agreed that the PM PiG would provide LADCO and the MRPO with an important advance in modeling technology to meet the regulatory goals that are coming up. In response, ENVIRON proposed an approach to carry out that work, to include a design document (ENVIRON, 2004), necessary coding modifications, testing and evaluation, and a final report (this document).

At the time of our original proposal, initial development of the new full-chemistry PiG algorithm was completed for gas-phase chemistry but had undergone only basic testing. We decided that additional review and testing were necessary before releasing it for general use, and so the new PiG was not included in the May 2003 release of CAMx v4. Since then, the full-chemistry PiG has undergone significant improvement and testing, and additional capabilities have been incorporated.

The design document formed the basis for this final report and the CAMx v4.20 User's Guide section describing the updated PiG algorithm. The objectives of the design document were to:

1. Describe the current formulation/status of the new full-chemistry PiG option;
2. Propose an approach for incorporating PM chemistry and deposition into that version of the PiG code; and
3. Identify available LADCO/MRPO modeling databases that can be used to evaluate the revised PiG algorithm.

The proposed approach described in the design document was reviewed by the MRPO and finalized for implementation.

1.1 BACKGROUND

In 2002/03, ENVIRON developed a new PiG model that includes full gas-phase chemistry (CB4 or SAPRC) to simulate the chemical evolution of NO_x and/or VOC point source plumes. The physical representation of plume segments (i.e., growth, dumping criteria, mass distribution, etc.) was updated to accommodate the full chemistry. Chemical processes are simulated within each plume segment using an "incremental chemistry" approach where puffs carry the incremental contributions of the puff relative to the grid concentrations. Incremental puff concentrations can be positive or negative, depending upon the species and stage of plume evolution. A similar chemistry approach is used in the SCICHEM Lagrangian model (EPRI, 2000) and in the Advanced Plume Treatment (APT) that joins SCICHEM to CMAQ. The name given to the new CAMx plume treatment is the IRON PiG (Incremental Reactions for Organics and NO_x). The original CAMx GREASD PiG is retained as a separate option.

In 2003/04 the IRON PiG was significantly restructured to: tighten up the original code for incremental chemistry, puff dynamics and dumping, etc.; to include improved puff expansion rates based on second-order closure methods; to add the capability to track reactive tracers (RTRAC); and to add high-resolution sampling grids to output and visualize plume concentrations of the reactive tracers. Also, the IRON PiG was strenuously tested for a number of configurations to ensure proper execution for both full photochemistry and reactive tracers. Section 2 of this report documents the current formulation of IRON PiG in detail. The IRON PiG will be released to treat ozone only in CAMx version 4.20.

The current IRON PiG is a solid foundation for a PM PiG model and we did not anticipate any major conceptual problems in extending IRON PiG to include PM chemistry. Section 3 of this report documents the updates we made to the current formulation of IRON PiG to incorporate PM chemistry and deposition processes for all species. However, further testing will be necessary to ensure correct implementation and to evaluate performance. The testing can be designed to consider performance for both ozone and PM and thus bring the IRON PiG with PM chemistry to the stage where it is ready for public release. Section 4 provides some guidance into how to evaluate PM PiG.

The original CAMx GREASD PiG model works with the OSAT ozone source apportionment technology. This was possible because of the simplified approach used in GREASD PiG and because compatibility with OSAT was an explicit design objective. GREASD PiG does not include any PM treatment, so it does not include PSAT. The incremental chemistry technique incorporated into IRON PiG, along with the puff-grid mass transfer constructs, are sufficiently complex that it would be very difficult to implement OSAT and PSAT within IRON PiG.

2. THE CAMx IRON PiG

The CAMx Plume-in-Grid (PiG) model was updated to incorporate several technical advancements. The primary goal was to include a more complete treatment of chemistry in point source pollutant plumes, while secondarily improving puff-grid mass exchange and adding additional features central for treating toxic pollutants not normally carried by the standard CAMx chemical mechanisms. The new PiG treatment is based on the philosophies used in the SCICHEM model, in that it incorporates non-linear “incremental chemistry” techniques and “second-order closure” methods for calculating the physical evolution of each puff.

Specifically, five major improvements were incorporated:

- An incremental full-chemistry approach called the Incremental Reactions for Organics and NO_x (IRON) PiG.
- Second-order closure puff dispersion parameterizations within both IRON and GREASD versions of the CAMx PiG.
- Reconfigured puff structure, revised dumping and mass exchange criteria/techniques, and a puff “rendering” capability in IRON PiG, all of which stemmed from the chemistry and dispersion improvements above.
- Tracking of specific chemical tracers (via RTRAC) within the IRON PiG, as well as after puff dumping into the computational grid; this adaptation permits the explicit treatment of tracer chemical decay, formation and decay of secondary/daughter compounds, and source apportionment.
- Plume/puff concentration sampling and rendering of RTRAC tracer species to a high-resolution receptor grid.

The GREASD PiG, with the improved second order closure dispersion treatment, is retained in CAMx as a separate option.

Below we describe the IRON PiG in detail as currently implemented in CAMx v4.20. The implementation of RTRAC components into IRON PiG was described in the design document, but since RTRAC is not central to the PM PiG, it is not repeated here.

2.1 BASIC PUFF STRUCTURE AND DIFFUSIVE GROWTH

Both GREASD and IRON PiG sub-models share a common basic structure and growth algorithm. A stream of plume segments (puffs) is released from a designated point source. Each puff possesses a longitudinal length and directional orientation defined by the separation of a leading and a trailing point. Initial separation of these points is determined by the wind vector at final plume rise, and each point is then subsequently and independently transported through the gridded wind fields. Like other puff models, the shape of each puff is characterized by a spread tensor, which is defined from a set of Gaussian standard deviations (so-called “sigmas”) along the three spatial axes (σ_x , σ_y , σ_z). Diffusive growth is defined by the growth in these sigma values.

We have developed an explicit solution approach for puff growth that shares SCICHEM theory and concepts (EPRI, 2000), but includes some simplifications. SCICHEM solves predictive spatial moment equations with second-order closure that relate the evolution of the puff spread tensor ($\sigma_{ij} = \sigma_i \times \sigma_j$) to resolved mean shears and turbulent velocity statistics. The Reynolds-averaged second-moment transport equation is given as

$$\frac{d\sigma_{ij}}{dt} = \sigma_{ik} \frac{\partial \bar{u}_j}{\partial x_k} + \sigma_{jk} \frac{\partial \bar{u}_i}{\partial x_k} + \frac{\langle x'_i \overline{u'_j c'} \rangle}{Q} + \frac{\langle x'_j \overline{u'_i c'} \rangle}{Q}$$

where \bar{u} is the mean wind vector component, the primed values represent turbulent fluctuations from the mean, and the angle brackets denote integrals over space. The Reynolds averaging process always introduces higher-order fluctuation correlations, and this is given by the turbulent flux moments $\langle x' \overline{u' c'} \rangle$, where $\overline{u' c'}$ represents the turbulent flux of concentration. It is these last two diffusion terms that SCICHEM solves in its second-order closure scheme.

For sub-puff scale turbulence, SCICHEM employs the restriction that the only off-diagonal component of $\langle x' \overline{u' c'} \rangle$ to be considered is the symmetric horizontal term ($i=x, j=y$), and then only for the large-scale (meso to synoptic) contribution to puff deformation when puff scale reaches such dimensions. In CAMx, we ignore this off-diagonal flux moment term altogether since puff mass is ultimately introduced to the grid when puff size is at the grid scale (1-50 km in practically all applications), and thus puffs never reach spatial scales at which this term becomes important. SCICHEM also makes the assumption that the horizontal turbulence is isotropic, $\langle x' \overline{u' c'} \rangle = \langle y' \overline{v' c'} \rangle$. This results in a single diffusivity equation for both x and y directions, and a single diffusivity for the z direction:

$$K_x = K_y = \frac{\langle y' \overline{v' c'} \rangle}{Q}$$

$$K_z = \frac{\langle z' \overline{w' c'} \rangle}{Q}$$

In our approach for CAMx, we have adopted the SCICHEM second-order tendency equations to model the time-evolution of puff turbulent flux moments (represented by diffusivities $K_x=K_y$ and K_z) and their contribution to the evolution of puff spread (represented by the diagonal components of the puff spread tensor, $\sigma_x^2 = \sigma_y^2$ and σ_z^2). Note that we ignore the off-diagonal contributions to puff spread, since they are unnecessary in the context of the CAMx PiG. Puff spread is defined for puff depth (σ_z) and puff width (σ_y); the latter is also added to the longitudinal length to allow for diffusive growth along the puff centerline. We account for the effects of wind shears in the evolution of lateral spread, but assume that the evolution of vertical spread is solely the result of turbulent fluxes.

The resulting two Reynolds-averaged second-moment transport equations for CAMx PiG are:

$$\frac{d\sigma_z^2}{dt} = 2K_z$$

$$\frac{d\sigma_y^2}{dt} = 2\sigma_y^2 D + 2\sigma_y \sigma_z \left(\frac{du^2}{dz} + \frac{dv^2}{dz} \right)^{1/2} + 2K_y$$

where D is deformation of horizontal wind.

The SCICHEM tendency equation for the horizontal turbulent flux moment is

$$\frac{d}{dt} \langle y'v'c' \rangle = Qq^2 - A \frac{q}{\Lambda} \langle y'v'c' \rangle$$

where $A = 0.75$, $q^2 = \overline{v'v'}$, and Λ is the horizontal turbulent length scale. Separate equations are given for two different boundary layer turbulence scales (shear- and buoyancy-produced), such that

$$\langle y'v'c' \rangle = \langle y'v'c' \rangle_{shear} + \langle y'v'c' \rangle_{buoyancy}$$

Within the surface-based boundary layer, the horizontal velocity variance is given by

$$q_{buoyancy}^2 = 0.13 w_*^2 [1 + 1.5 \exp(z / z_i)]$$

$$q_{shear}^2 = 2.5 u_*^2 (1 - z / z_i)$$

where u_* is the friction velocity, w_* is the convective velocity scale, z is height above the surface, and z_i is the height of the surface-based boundary layer. The horizontal turbulent length scale is given by

$$\frac{1}{\Lambda_{shear}^2} = \frac{1}{(0.3 z_i)^2} + \frac{1}{(0.65 z)^2}$$

$$\Lambda_{buoyancy} = 0.3 z_i$$

In the stable boundary layer, only the shear components of q^2 and Λ are applied. Above the boundary layer, SCICHEM applies rough approximations for the velocity variance and turbulent length scale: $q^2 = 0.25 \text{ m}^2/\text{s}^2$, and $\Lambda = 1000 \text{ m}$.

The SCICHEM tendency equation for the vertical turbulent flux moment is

$$\frac{d}{dt} \langle z'w'c' \rangle = A \frac{q_v}{\Lambda_v} \left(QK_z^{eq} - \langle z'w'c' \rangle \right)$$

where $q_v^2 = \overline{w'w'}$, Λ_v is the vertical turbulent length scale, and K_z^{eq} is the equilibrium diffusivity. Whereas a specific equation for K_z^{eq} is formulated for SCICHEM, we have chosen to specify the value of this parameter from the gridded fields of vertical diffusivity in CAMx. Again SCICHEM gives separate equations for shear- and buoyancy-produced turbulence scales.

Within the surface-based boundary layer, the vertical velocity variance is given by

$$q_v^2 \Big|_{shear} = 1.5 u_*^2 (1 - z / z_i)$$

$$q_v^2 \Big|_{buoyancy} = 1.1 w_*^2 (z / z_i)^{2/3} (1.05 - z / z_i)$$

The vertical turbulent length scale for both shear and buoyancy is equal to Λ_{shear} given above for horizontal length scale. Above the boundary layer, SCICHEM again applies rough approximations for the velocity variance and turbulent length scale: $q_v^2 = 0.01 \text{ m}^2/\text{s}^2$, and $\Lambda_v = 10 \text{ m}$.

The external variables needed by IRON PiG to complete the dispersion calculations include z_i , u_* and w_* . All of these are available from an internal module in CAMx that calculates these boundary layer similarity theory parameters. Thus, no additional parameters are needed to be input to the model.

2.2 PUFF TRANSPORT

A fresh set of new puffs are released from all PiG point sources within the modeling domain for the duration of the smallest time step among the master and all nested grids. The length of each puff is determined by the combination of the mean total wind speed at the height of final plume rise and time step. Limits are placed on maximum extruded length based on half the finest resolution in the given simulation. If winds and time-steps are such that the maximum allowed length is violated, then several puffs are extruded from a given stack per time step. The orientation of the puff length is along the total wind vector. Total puff volume is determined by stack volumetric flow rate in conjunction with growth due to turbulent entrainment following the SCICHEM approach. Initial σ_y and σ_z are explicitly calculated from this entrainment calculation.

Effects of wind divergence on plume deformation are treated in an explicit manner within the CAMx PiG using a "chained puff" approach. Points at the leading and trailing edges of the puff centerline are individually transported through the gridded wind fields, which directly accounts for puff stretching and changes to centerline orientation due to deforming shears. Since IRON PiG puffs can extend over multiple layers, layer density-weighted average wind components are determined for each endpoint based on the vertical coverage of the puff, and these are used for advection of those points. GREASD PiG puffs are not allowed to expand beyond the depth of the layer in which the center point resides, so only the single layer wind components are used to advect the end points.

The "chain" aspect means that at least initially (as puffs are extruded from the stack) the trailing point of a puff emitted at time t will be the leading point of a puff emitted at time $t+dt$. However, as the puffs are advected downstream, the leading point of one puff will deviate from the trailing point the puff behind it due to evolving puff size and wind fields. Puff volume is conserved in convergent/divergent wind fields. Puff endpoints may move closer together or further apart, in wind fields that are slowing or accelerating downstream. We compute puff endpoint separation changes and then adjust puff widths and depths to maintain constant puff volume. The change in computed puff endpoint spacing defines puff length tendencies, then puff

depth tendencies are computed from grid-resolved vertical wind shear (dw/dz), and finally we determine the puff width tendencies required to conserve puff volume.

The official "position" of each puff is defined by the center point of each puff between the endpoints. This position defines which grid domain and grid cell the puff resides for the calculation of diffusion and chemistry. This definition holds even if the puff is sufficiently long that the endpoints are in different grid cells (or even different grid domains if near a domain boundary). With our definition for termination when horizontal area approaches grid cell area, the extents of the puff length should not extend across more than two grid cells.

2.3 MODIFICATIONS SPECIFIC TO IRON PiG

The IRON PiG model incorporates several technical advancements. The primary goal was to include a more complete treatment of chemistry in point source pollutant plumes, while secondarily improving puff-grid mass exchange and adding additional features central for treating toxic pollutants not normally carried by the standard CAMx chemical mechanisms. Several approaches have been developed to treat photochemistry within point source plume models. One of the more elegant methodologies is the incremental chemistry idea embodied in the SCICHEM model (EPRI, 2000). However, we found that the implementation of incremental chemistry in SCICHEM is very complex, especially in its handling of the chemistry of overlapping puffs. In adopting this innovative approach for the IRON PiG, it was necessary to reformulate the physical and chemical configuration of the PiG puffs, and to utilize a robust numerical solution approach based on the LSODE chemical solver.

The Concept of Incremental Chemistry

For a second-order reaction between puff species A and B , the total reaction rate is the following:

$$R_T = k(P_A)(P_B) \quad (1)$$

where P_A and P_B are the total puff concentrations of each species. The total puff concentrations can be expressed as the sum of the background and puff perturbation concentrations in:

$$P_A = (c_A + C_A)$$

$$P_B = (c_B + C_B)$$

where C is the ambient concentration and c is the puff increment concentration. Thus the reaction rate is found to be:

$$R_T = k(c_A + C_A)(c_B + C_B)$$

or

$$R_T = k(c_A c_B + C_A c_B + c_A C_B + C_A C_B)$$

If we subtract the rate of change of the background,

$$R_{Ambient} = C_A C_B \quad (2)$$

by assuming that it is explicitly and separately treated by the grid model, we obtain the reaction rate for the puff increments:

$$R_p = k(c_A c_B + C_A c_B + c_A C_B) \quad (3)$$

Equation 3 is the basis of SCICHEM incremental chemical kinetic solver. One problem with this approach is the mixed terms, $C_A c_B$ and $c_A C_B$. Most chemical solver packages are designed to solve rate equations for total concentration, as in Equation 1. Thus, for the IRON PiG we developed an alternative numerical solution scheme for puff perturbation chemistry. We note that the CAMx chemical solver can be independently applied to the rate equation for total puff concentrations, Equation 1, and to the rate equation for ambient concentrations, Equation 2. By subtraction of the two solutions, we obtain the solution to rate Equation 3. This requires no modification to, and is obviously completely self-consistent with, the CAMx chemical solvers. Once the incremental puff reaction rates are obtained they are applied to the incremental puff mass to calculate the new (adjusted for chemistry) incremental concentrations. These new puff increments are subsequently advected and dispersed by the transport portions of the PiG code.

Puff Constructs For Incremental Chemistry

The IRON PiG sub-model includes three new constructs designed specifically to facilitate the incremental chemistry approach:

- Treatments to handle puff-grid information exchange for puffs spanning multiple model layers;
- The concept of “virtual dumping” to handle the chemical impacts of large puffs that can overlap other puffs within a given grid column;
- The concept of multiple puff “reactor” cells to account for the chemical effects of concentration distributions within each puff.

Each of these are described below.

Puff Layer Spanning

The IRON PiG is designed to chemically process point source plume mass within streams of puffs until such time that each puff can be adequately resolved on the *horizontal* grid. Unlike the GREASD PiG approach, where the vertical layer structure dictates puff leaking and ultimately termination, the approach in IRON PiG leads to the necessity that puffs be allowed to vertically span multiple grid model layers before they reach horizontal grid scales. This introduces technical implications for defining “background” concentrations and ambient conditions for puff chemistry, as well as for transferring plume incremental mass to the grid. The solution employed in IRON PiG is to:

1. Assume that the vertical distribution of puff concentration is always uniform;
2. Distribute puff mass transfer (via “leaking” and “dumping”) to the grid according to the puff fractional coverage across each model layer and by density-weighting; and

3. Determine mean background concentrations and other ambient conditions (e.g., temperature, humidity, etc.) over the puff vertical span via similar fractional layer-density weighting.

IRON PiG puffs are considered to be elliptical in the horizontal, with the minor axis spanning the crosswind puff width (defined as $\pm 1.5\sigma_y$), and the major axis spanning the along-wind puff length (defined as length $\pm 1.5\sigma_y$ on each end). This is similar to GREASD PiG. However, given the complications associated with multiple layer spanning and mass-weighting of ambient inputs and dumped mass, IRON puffs are rectangular and uniform in the vertical, with total puff depth defined as $\pm 1.5\sigma_z$.

Horizontally, the mean background concentration and ambient conditions are taken from the single host grid column containing each puff center point, even if the puff is large and/or spans a horizontal cell interface.

Puff Overlap and the Idea of Virtual Dumping

The chemical effects of puff overlap were considered to be an important attribute of IRON PiG. However, we wished to maintain a relatively simple approach, while appropriately accounting for the largest probable effects. We assume that the largest effect is the condition in which older expansive puffs span significant fractions of their host grid cell, thereby potentially overlapping all other puffs contained within the same cell. Instead of geometrically determining fractional overlap puff-by-puff, we instead introduce a process that we refer to as “virtual dumping.”

For a given grid column, the mass from all puffs determined to be “sufficiently” large are temporarily dumped to the column, distributed according to each puff’s vertical layer span, and added together along with the pre-existing grid concentrations. This process is referred to as a “virtual dump” of puff mass to the grid column. The criteria to determine a “sufficiently” large puff is the same that initiates puff mass leaking to the grid (as described below). In this approach, all large puffs contribute to the background chemistry step for other puffs occupying the same grid column. Double-counting of chemistry is avoided by not including a puff’s contribution to the background while it’s specific background and incremental chemical calculations are performed.

Multiple Puff Reactors

Accounting for full chemistry potentially introduces significant non-linear effects that are highly dependent upon the distribution of pollutant mass within each puff. Especially for ozone, aircraft flights through power plant plumes have often recorded wide concentration variations relative to ambient conditions: within the plume core where NO_x remains concentrated, ozone is often depressed and follows NO-NO₂-ozone equilibrium, whereas on plume fringes where NO_x is dilute and mixes with ambient VOC, ozone concentrations can exhibit concentration maxima. Past models have accounted for cross-plume chemistry variations through the use of reactors, with approaches ranging from multiple rectangular slabs to concentric shells.

In IRON PiG, the user may select multiple reactors as well to sub-divide the puff. Any number of reactors may be chosen (the default is 1). Multiple reactors simply divide the total puff

volume evenly, and the initial mass assignments for newly emitted puffs are made using the standard error function that results in an initial Gaussian-like mass/concentration distribution among the reactors. This provides a mechanism for simulating the differing chemical processing that takes place in various concentration regimes. As the purpose of the reactors is merely to represent the range of photochemical conditions that are likely to occur at various locations within the puff as it undergoes differential shearing and mixing, there is no particular physical orientation assigned to these reactors with respect to each other or to the puff as a whole. Thus, there is no communication (i.e., diffusional mass exchange) between the reactors. The same background concentration chemistry applies to all reactors of a given puff. When puff mass is leaked or dumped, all reactors shed the same relative fraction of mass.

In summary, chemistry is solved for each IRON puff “reactor” in three steps:

- 1) The layer-mean background (grid + overlapping puff) concentrations and environmental conditions over the volume occupied by the puff are stored and then chemically updated via the LSODE gas-phase chemistry mechanism;
- 2) The pre-updated mean background concentrations are added to the puff increments and the total concentrations are chemically updated; and
- 3) The updated results from step 1 are subtracted from the updated results of step 2 to provide the updated incremental concentrations.

An important consequence of this approach is that the incremental puff mass may be positive or negative. For example, a high-NO_x puff that is destroying ambient ozone will have negative ozone increments. The puff increments are subsequently advected and dispersed by the transport portions of the IRON PiG code. Note that the updated background concentrations, which include “virtual dumps” of mass from large puffs, are used for reference only in the puff incremental chemistry algorithm; the actual grid concentrations are updated in the grid chemistry routine.

IRON Puff Dumping and PiG Rendering

Mass transfer from puff to grid can happen in two ways: slowly, termed “leaking”, or suddenly, termed “dumping.” As described earlier, all mass is transferred to the vertical grid structure in a density-weighted fashion according to each puff’s fractional layer coverage. The process of leaking ensures that puff mass is transferred to the grid continuously, rather than in discrete lumps of pollutants with very different concentrations than those in the grid. Sudden dumping can cause unphysical numerical shocks in the grid and can lead to unrealistic gridded concentration patterns that appear as “bullseyes”. The idea behind puff leakage is to account for turbulent shearing of mass from the main plume and its subsequent dispersion to the grid scale. This rate of transfer should be directly proportional to the puff size relative to the grid scale.

Puff leakage is controlled by comparing the horizontal area of a puff to a specified leakage parameter, defined as a fraction of horizontal grid cell area. When a puff is first emitted there is no leakage. As the puff grows in volume the concentrations within the reactors are reduced accordingly by dilution. When the puff area exceeds the leakage onset parameter, a fraction of the mass in each puff reactor is transferred to the grid. This fraction is determined by the relative exceedance of the leakage parameter; initial leakage is slow as the exceedance is relatively small, but leakage rates grow as the puff continues to grow beyond the leakage parameter.

Like GREASD PiG, the reduced mass from leakage is compensated by a reduced effective volume, so that concentrations are not artificially diluted by leakage (an essential chemical imperative). Thus, two distinct volumes are tracked: the actual volume (defined by the puff spread sigmas) and the effective volume. While these are identical before leakage, they obviously deviate after leakage is initiated, and thereafter the relative deformation of the actual puff volume (via diffusion, shearing, etc.) is used to scale the deformation of effective puff volume.

Eventually the horizontal span of the puff will exceed the grid cell area, and the remaining mass is then dumped all at once to the grid. However, because of the combination of photochemical processing and leakage, by the time a puff dumps the potential for producing numerical shocks is much reduced. Furthermore, if the puff exceeds a user-defined maximum age, puff mass is transferred to the grid at the rate of 10% per time step (as in GREASD PiG).

While the mass confined to the puffs at any given time has not yet affected the grid concentrations, it will eventually, so it can be somewhat misleading not to include it in visualizations of a model simulation. The puff mass can be optionally incorporated into the model average output files for visualization purposes (referred to as "PiG rendering"). Rendering employs a "virtual dump" of the puff masses into the average concentration array each time step. As described for chemistry, virtual puff mass is added as an increment over the entire grid column according to fractional layer-density weighting over puff depth, thus diluting its concentrations relative to that within the puff. The actual puff mass remains within the puffs over the course of their lifetimes. It should be noted that this visualization is available for 3-D average output files, and can produce some rather startling effects in output displays, including very narrow virtual plumes, or streaks, representing mass moving through the grid in sub-grid puffs, but not subject to grid-scale eddy diffusion.

3. IMPLEMENTING PM CHEMISTRY AND DEPOSITION INTO IRON PiG

The physical representation of plume segments developed for treating ozone photochemistry within the IRON PiG were found to be equally appropriate for PM. Furthermore, the approach to implement PM chemistry into the IRON PiG closely paralleled the approach for grid chemistry, by calling the same ISORROPIA, SOAP and RADM-AQ modules in the same order and manner. However, these PM chemistry modules are called for each puff using the same incremental chemistry approach that IRON PiG uses for the gas-phase ozone chemistry; i.e., by separate integrations for background and puff+background in order to determine the evolution of puff incremental concentrations. Note that the PM PiG was designed specifically for the CF version of PM chemistry only, not for the CMU PM chemistry.

The PM PiG updates developed over the past year were adapted to and incorporated into the pre-release version of CAMx v4.20 (this version is referred to as v4.20_PMPiG). As stated earlier, the official release of v4.20 will not include these PM updates in IRON PiG since only preliminary testing has been conducted at ENVIRON for this latest incarnation.

3.1 PM CHEMISTRY

The IRON PiG performs chemical calculations for a given puff over each time step of the host grid where the puff resides. This is done by calling a chemistry driver routine that is practically identical to the grid chemistry driver, except that layer-averaged ambient conditions over puff depth are passed to the chemistry algorithms rather than cell-specific conditions. The driver routine contains the specific calls to all supported CAMx chemistry mechanism solvers, including the CF PM algorithm. The process of including the PM mechanisms was relatively straightforward. The calls to the gas and aerosol solvers were updated to pass the appropriate layer-averaged ambient conditions needed for PM chemistry consistent with the current version of the CF PM mechanism in CAMx v4.20. The chemistry driver routine for grid concentrations was the basis for this update.

However, one important change was made from the PM chemistry implementation of v4.20, and this affects both the grid and PiG puff chemistry. In v4.20 (and earlier), both the CF and CMU algorithms are called at the PM “coupling” steps. The time interval between coupling steps is normally set to 15 minutes within the chemistry parameters file. The purpose of the coupling interval is to reduce the frequency of calls to the rather demanding ISORROPIA routine, rather than calling it every time step, to maximize speed performance. In testing v4.11s and v4.20, we had noticed some sharp differences in PM concentrations along nested grid boundaries that crossed through cloudy regions – it appeared that entirely different chemistry was occurring on either side of these boundaries. Our investigations revealed that this is largely caused by inconsistencies in the time at which the aqueous PM chemistry algorithm is called for each grid. The PM coupling step can result in a different number of aqueous chemistry (and ISORROPIA/SOAP equilibrium) calls per hour, and/or different time step lengths for the chemistry integration, for each grid. For example, suppose the master time step on the 36-km grid is 10 minutes, and the time step on the 12-km grid is 5 minutes. With a 15 minute coupling interval, PM chemistry is called for the 36-km grid at 20, 30, 50, and 60 minutes past the hour (with aqueous integration time steps of 20, 10, 20, and 10 minutes), whereas PM chemistry is called for the 12-km grid at 15, 30, 45, and 60 minutes (all 15 minute aqueous time steps). This

can exacerbate differences in output hourly average PM concentration fields between 2 or more nested grids.

To diminish the impact of grid-dependent chemical inconsistencies, we modified the PM PiG version of CAMx to call the aqueous PM chemistry algorithm at every time step for each grid. This is done for both grid and puff chemistry. The remainder of the PM chemistry (ISORROPIA and SOAP) continues to be called on the 15 minute coupling time step, as these routines are not based on integrating conversion rates, but rather are equilibrium calculations independent of time step. This also continues to maximize CAMx run time efficiency as ISORROPIA requires the most amount of CPU time to be solved and would therefore slow the model considerably if it were to be called every time step.

3.2 DRY AND WET DEPOSITION

Deposition of gas and PM species were also added to the PM PiG algorithm. Both dry and wet deposition calculations presented unique implementation issues for puffs. The most difficult issue for both forms of deposition was how to manage deposition exchange between puffs and the ground in the case of negative puff concentration increments. This and other issues that we had anticipated in the planning stages of this project were discussed in detail in the design document (ENVIRON, 2004).

Dry Deposition

Dry deposition needed to consider the following: (1) the point at which puffs begin to deposit to the surface; (2) how to handle deposition through potentially deep puffs that may straddle several layers of varying stability since the puffs do not themselves resolve these stratifications or vertical concentration distributions; (3) managing deposition fluxes of negative concentration increments. Our solution to issue (1) was to ignore dry deposition within puffs until they diffusively grow to the ground, although deposition occurs on roughness elements that extend some distance above the nominal surface (trees, buildings, etc.). The heights of puff bottom and top are tracked in terms of distance above ground, so it is easy to identify when plumes reach the surface. We implemented a criterion that the bottom of the puff must extend to or below the midpoint of the surface layer, or below 10 m (whichever is larger), in order for dry deposition to be active.

Issue (2) can be handled in a variety of ways and complexity. At this point we aimed to institute simpler solutions and will consider more complicated improvements for future developments if evidence suggests that they would be necessary. Our initial implementation utilizes pre-computed species-dependent deposition velocities derived for the grid. Each puff in a particular grid cell is provided the host cell's deposition velocities for each species, and these are used to determine the flux of mass through the fraction of puff depth occupying the model's surface layer.

Issue (3) is unique to the incremental chemistry concept introduced with IRON PiG. The flux of material depositing to the ground is given by $F = c \cdot v_d$, where by the normal definition a positive deposition velocity v_d leads to a positive deposition flux to the ground. If the puff increment c is negative, then a negative flux is calculated (flux from ground to puff). This is appropriate if we

consider the following argument. Dry deposition applied to a grid cell removes some pollutant mass from the entire volume. If there is a puff existing in that cell with a negative concentration increment, then the amount of mass removed from the cell was over estimated if we consider the puff's contribution to total cell mass. The negative deposition flux calculated for this puff leads to the addition of mass to the puff increment. Adding mass to a negative increment reduces the magnitude of the increment, as expected for a deposition process. This mass is taken from the grid cell's accumulated deposited mass to maintain accurate mass accounting within the model.

Wet Deposition

Wet deposition needs to consider the following: (1) how to handle scavenging of pollutants through potentially deep puffs that may straddle several layers of varying cloud and rain water contents but that do not themselves resolve vertical concentration distributions; (2) managing deposition fluxes of negative concentration increments in combination with the potential for mass to move in and out of rainwater as it falls (e.g., for slightly soluble gasses); (3) accounting for the initial pollutant concentrations in rainwater as they enter the top of each puff.

It was important to maintain consistency between the treatment of wet deposition and the approach for puff chemistry. The chemistry relies on the assumption of vertically well-mixed puff reactors that can span multiple layers, and this is why layer-density weighted average ambient conditions are passed to the chemistry routines. To maintain this assumption for wet deposition, a single scavenging rate is applied through the entire puff depth as effectively a single layer of pollutant. This was found to be the simplest implementation approach. This single scavenging rate is calculated according to layer-density weighted average ambient cloud and rainwater contents. Despite this simple implementation, a special wet deposition algorithm was needed for IRON PiG to handle the specific circumstances associated with the physical puff structure.

Wet scavenging is performed throughout the entire depth of the puff to determine the amount of flux in or out of rainwater. Total concentrations (puff + background) are used to determine species-dependent scavenging rates using the identical algorithm as for grid removal. The rates are used to derive removal fractions, and these fractions are then applied directly to the puff incremental mass for each species. Removal fractions are considered positive for the standard case of mass moving from puff to rain. Note that negative puff mass increments in combination with a positive removal fraction lead to a reversal of the flux direction (rain to puff), and that is acceptable by an argument similar to that presented for dry deposition. We account for impacts on the mass budget appropriately by adding or subtracting from the wet deposition mass array according to the net fluxes into and out of rainwater, respectively.

We further assume that the top boundary condition for rainwater entering the top of each puff is zero. This means that the removal fraction is always positive (from puff to rain) in the single-layer puff. In contrast, for gridded concentrations the layer-by-layer buildup of slightly soluble species can lead to a reversal of fluxes (from rain to grid) if super saturation is diagnosed in a particular layer. The effects of the zero initial condition assumption should be evaluated in future tests of the IRON PiG algorithm.

4. PRELIMINARY IRON PiG TESTING AND EVALUATION

4.1 SETUP

Preliminary testing of CAMx v4.20_PMPiG was conducted using the standard test case available on the CAMx web site (www.camx.com). This includes a 2-day (June 13, 14 2002), 2-grid (36-km and 12-km) simulation using inputs originally developed by the MRPO. The updated CF version of Mechanism 4 was employed, which includes new reactions for NO_x recycling and an additional 5th CG/SOA pair. The original point source file from the MRPO for these dates were modified to select 488 point sources that emit greater than 10 TPD NO_x. Note that even though our criteria for selecting PiG sources is based on NO_x, all chemical species emitted by these sources are carried within the PiG for ozone and PM chemistry and removal. The specifics of the simulation are provided in Table 4-1.

Table 4-1. Configuration of the preliminary PM PiG test case.

Simulation Dates	0000 EST 6/13/02 to 2400 EST 6/14/02
Map Projection	Lambert Conic Conformal
Projection Parameters	center lat/lon = -97/40, true lats = 33/45
Master Grid	97x90x14 36-km grid spacing origin = (900, -1620)
Nested Grid	119x134x14 12-km grid spacing master grid range = (31,29) to (69,72)
Chemistry Parameters	v4.2 Mechanism 4 CF
Environmental Inputs	Provided by MRPO
Emission Inputs	"BaseF"
PiG Sources	488 point sources emitting > 10 TPD NO _x
IRON PiG Configuration	Number puff reactors: 1 Puff leakage: off Puff rendering: on Puff overlap: off Max puff age: 18 hours

The run required over five CPU hours/day on a single-processor AMD Athlon MP 2800+ Linux PC (1 Gb memory, ~2100 MHz clock speed). OMP is not currently supported in the PM PiG version of CAMx.

The purpose of the setup described above was to maximize combinations of point source types and potential ambient environments in a single run to test the stability of the model code in a variety of situations. We anticipate that a typical application of IRON PiG will focus more on detailed research-level investigations on the evolution of pollutant plumes from a few key point sources of interest, rather than a broad-brush application as we have undertaken in the preliminary evaluation. User's of IRON PiG will find that the model does slow considerably for large number of PiG sources, since gas-phase chemistry is solved exclusively using the fully explicit LSODE solver, and both gas and PM chemistry are effectively solved twice per puff

(once for background, once for total puff) each time step. This is exacerbated by the use of multiple reactor cells per puff (the default is 1). Careful consideration should be given when defining each IRON PiG application.

4.2 EVALUATION

The plots that follow are provided to illustrate the impact of PM PiG on concentration fields of ozone, SO₂, individual secondary inorganic PM (sulfate, nitrate, ammonium), total secondary inorganic PM, and SOA. Impacts on SO₂ deposited mass from both dry and wet processes are also shown. Absolute concentration and deposition fields are shown from the run described above, with 488 PiG sources activated. Plots of differences in these fields are also provided, where the PM PiG run is differenced with a no-PiG run (same configuration otherwise). For brevity, we chose to plot the results at 1500 EST on the second day (June 14, 2002); readers should note that significantly different patterns and PiG impacts can be seen at other times of simulation.

Figures 4-1 and 4-2 display ozone at the surface and in layer 5 (this layer was chosen as the bulk of emissions from large point sources are lofted to this altitude). The difference plots in ozone clearly show the impact of the PiG algorithm at both elevations. All remaining concentration plots are shown for layer 5. Figure 4-3 shows the SO₂ precursor pattern; Figures 4-4 through 4-8 show sulfate, nitrate, ammonium, total secondary inorganics, and SOA, respectively. Note that the sources chosen for the PiG treatment were high in NO_x (and SO_x) emissions, and few emitted only low levels of the VOC precursors that evolve into SOA components. Hence, the SOA difference plot shows rather small impacts from PiG relative to the inorganic concentrations.

Finally, deposition loadings were briefly evaluated. Figures 4-9 through 4-10 show SO₂ dry and wet deposition, in terms of both absolute (from the PM PiG run) and differences from the no-PiG run. This species was chosen since large PiG impacts were seen in concentration fields, and because SO₂ removal is efficient for both dry and wet processes.

4.3 GUIDANCE ON TESTING PM PiG

Further testing of PM PiG is necessary to evaluate various PiG configurations over a broader range of potential mixtures of source types and ambient environments. We are forwarding the CAMx source code and a preliminary edition of the v4.20 User's Guide to LADCo so that the MRPO may design and undertake their own independent evaluations. Below we provide some additional information that is intended to assist future users of this particular version of CAMx to assess the results and performance of the PM PiG.

Review of the output average files is the most obvious starting point of any review. We suggest that to fully gauge plume impacts on the gridded average output, the PiG "rendering" flag be set to true (this is the default). This flag enables the "virtual" transfer of all PiG mass to the host grid cells during puff evolution so that their impacts can be visualized in the average output fields for the entire plume life cycle. The mass is not actually transferred from puffs to grid until certain conditions are met (this was described above, but we have added some additional dumping criteria for chemical stability, as described below). If the rendering flag is set to false,

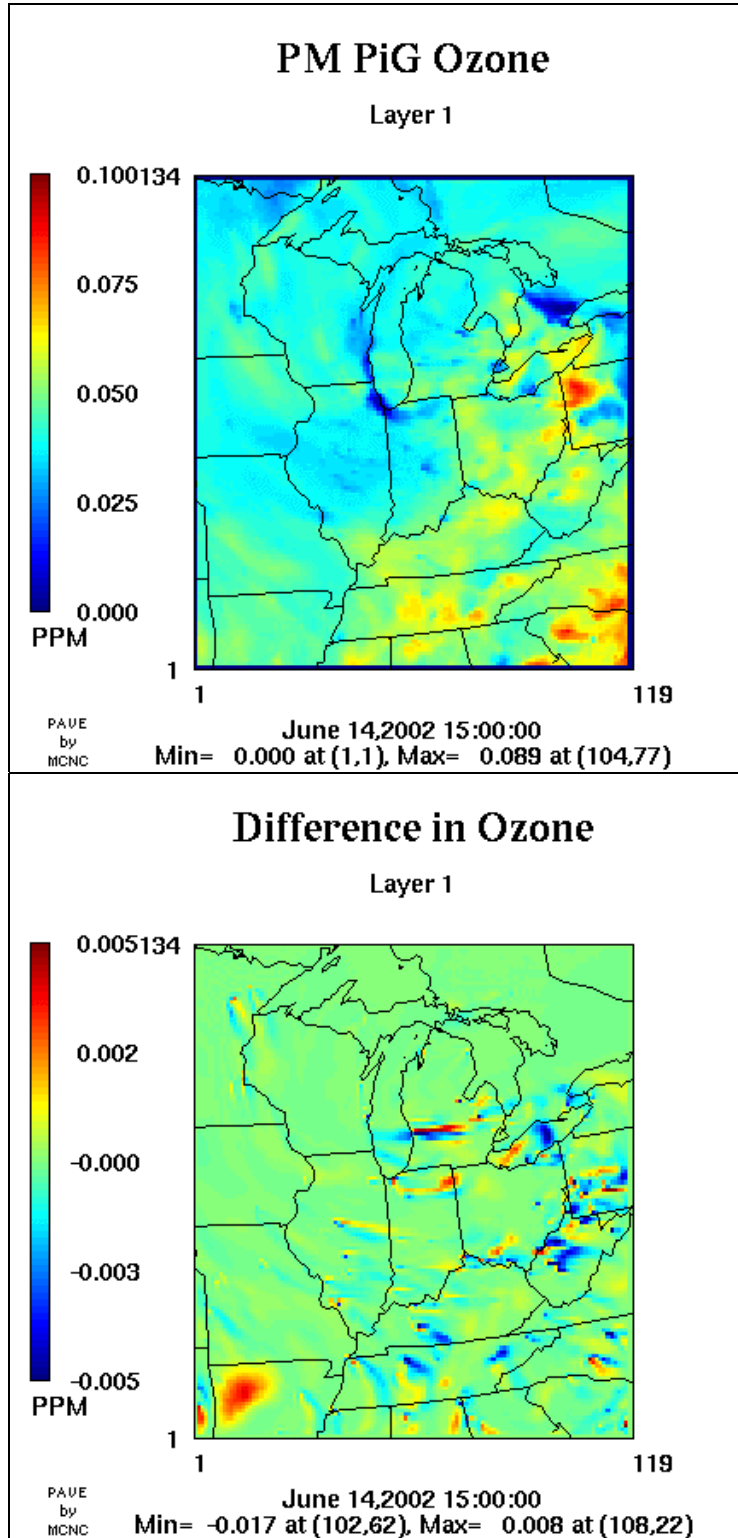


Figure 4-1. Ozone concentrations (ppm) in layer 1 for the PM PiG run (top) and for the difference between the PM PiG and no-PiG runs (bottom).

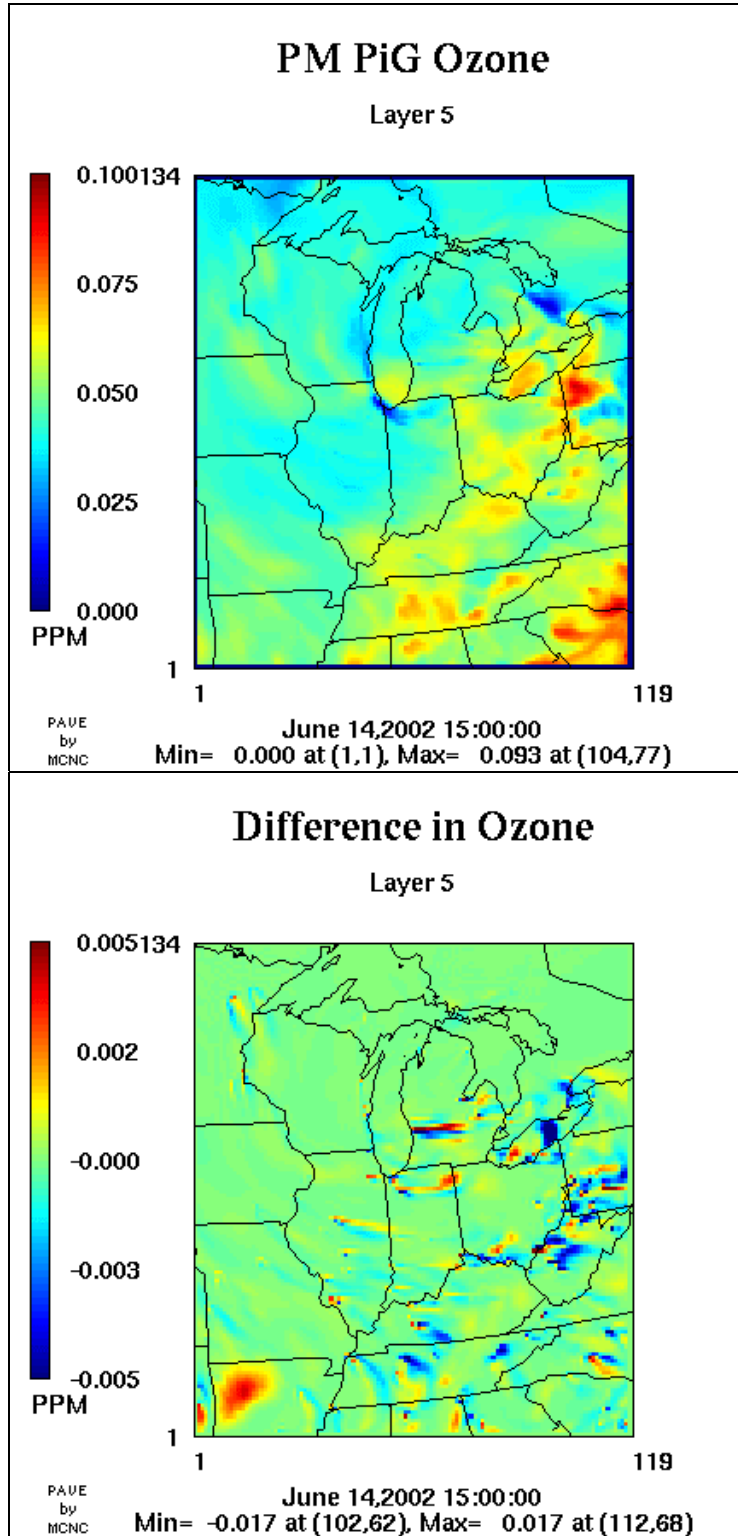


Figure 4-2. Ozone concentrations (ppm) in layer 5 for the PM PiG run (top) and for the difference between the PM PiG and no-PiG runs (bottom).

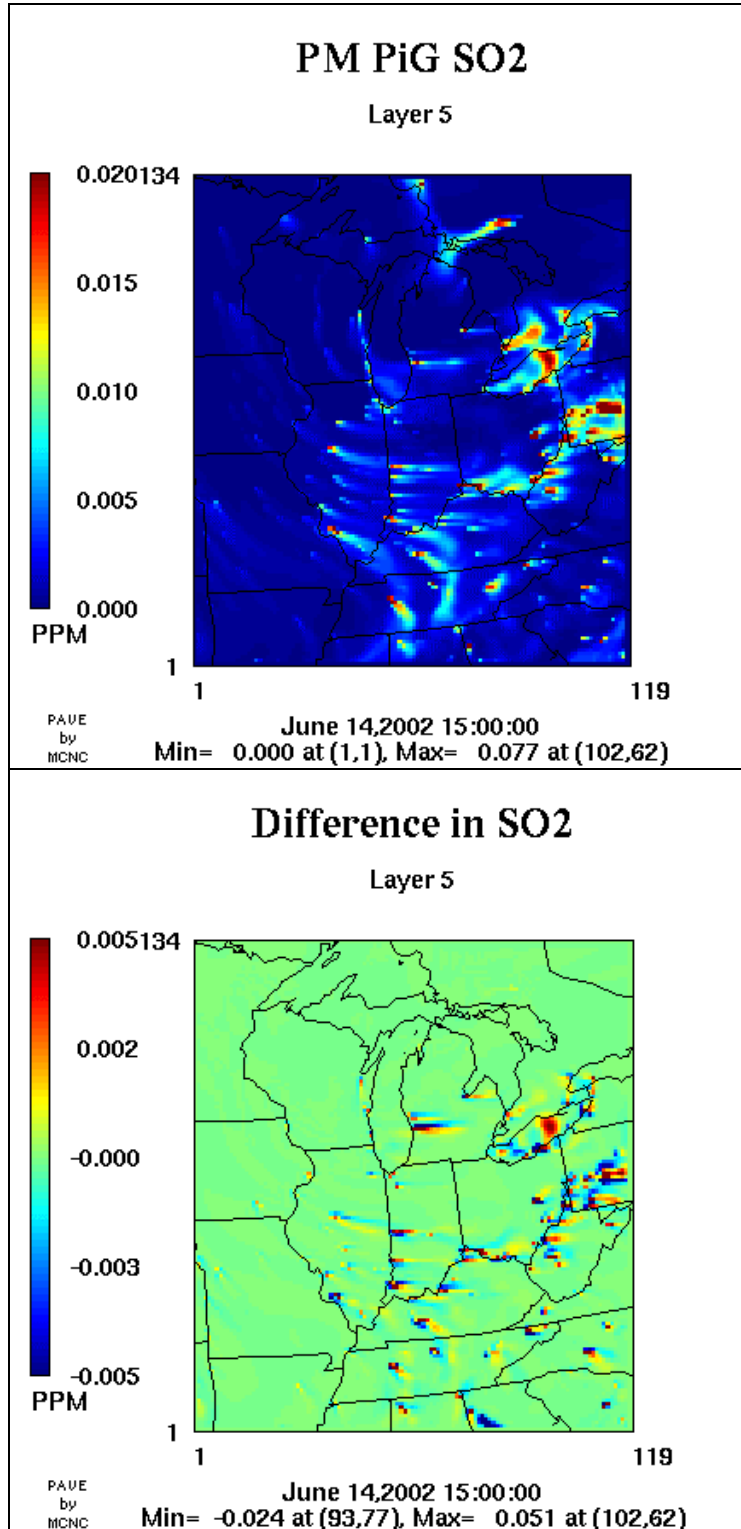


Figure 4-3. SO₂ concentrations (ppm) in layer 5 for the PM PiG run (top) and for the difference between the PM PiG and no-PiG runs (bottom).

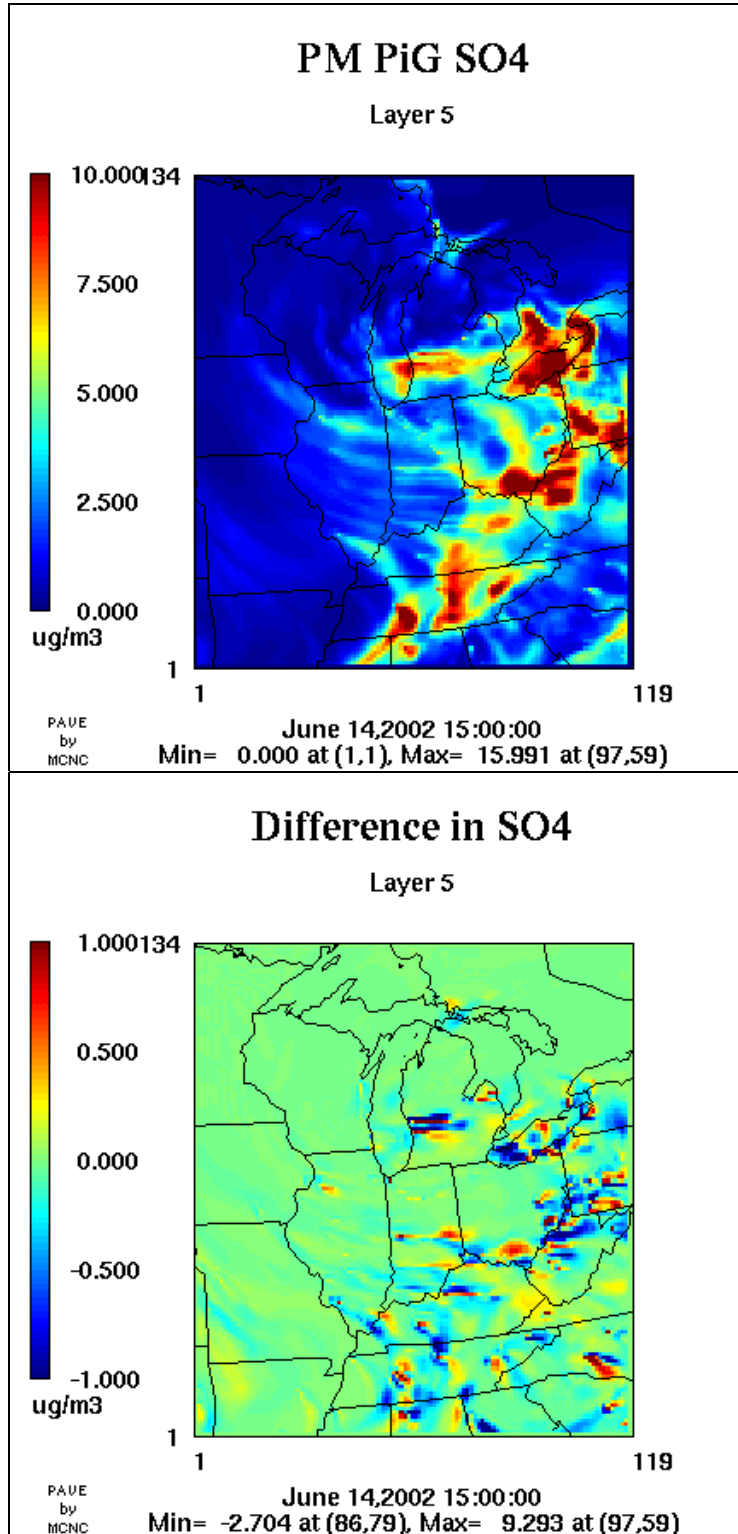


Figure 4-4. Sulfate concentrations ($\mu\text{g}/\text{m}^3$) in layer 5 for the PM PiG run (top) and for the difference between the PM PiG and no-PiG runs (bottom).

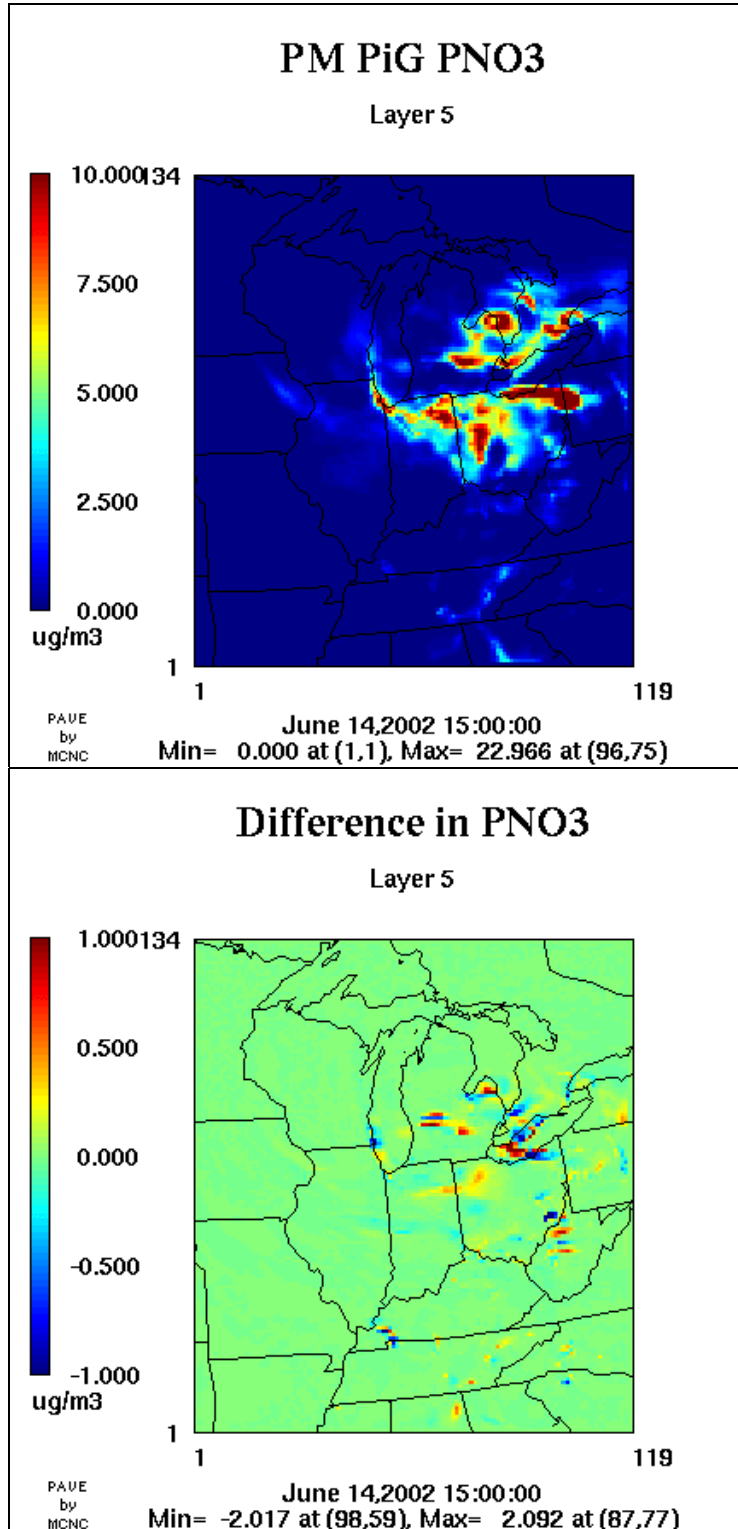


Figure 4-5. Nitrate concentrations ($\mu\text{g}/\text{m}^3$) in layer 5 for the PM PiG run (top) and for the difference between the PM PiG and no-PiG runs (bottom).

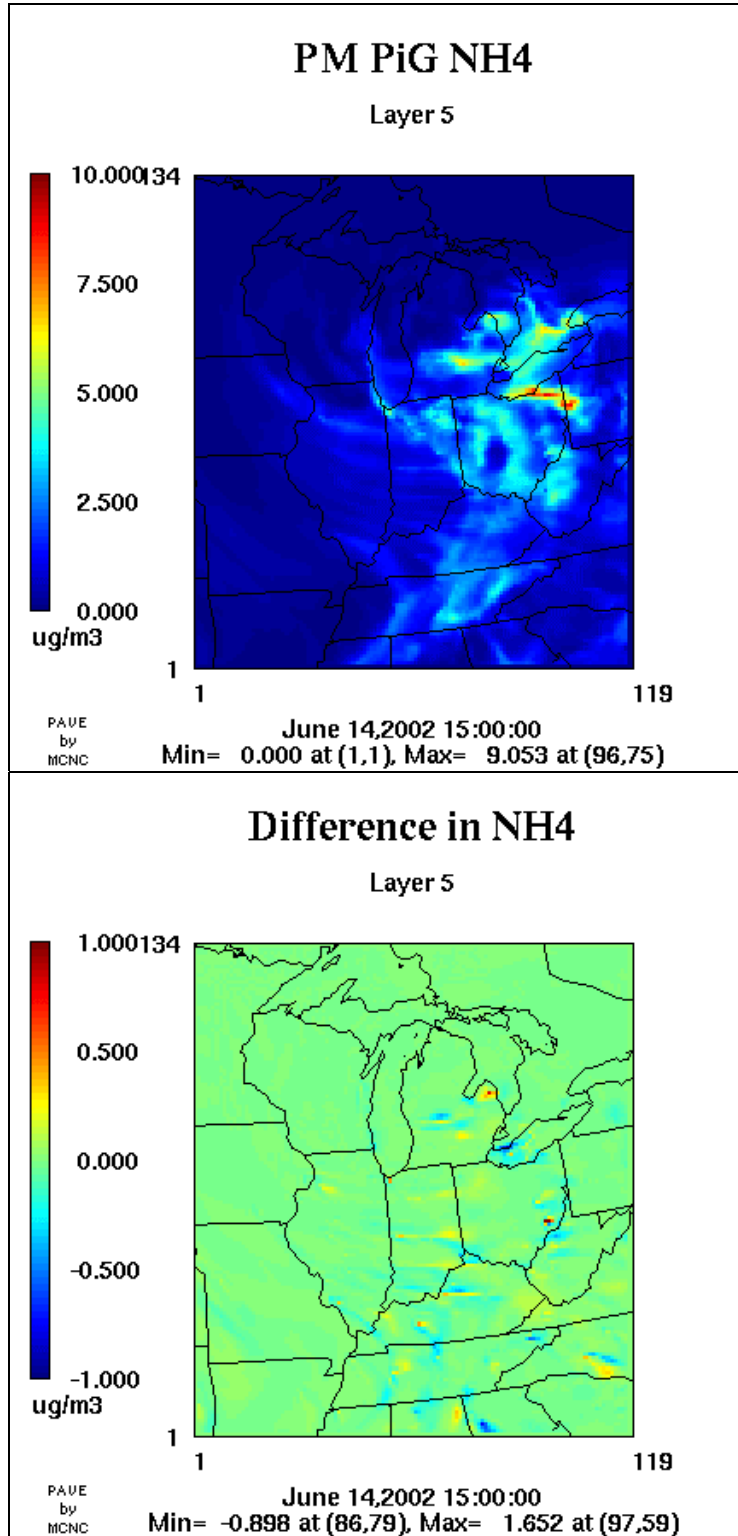


Figure 4-6. Ammonium concentrations ($\mu\text{g}/\text{m}^3$) in layer 5 for the PM PiG run (top) and for the difference between the PM PiG and no-PiG runs (bottom).

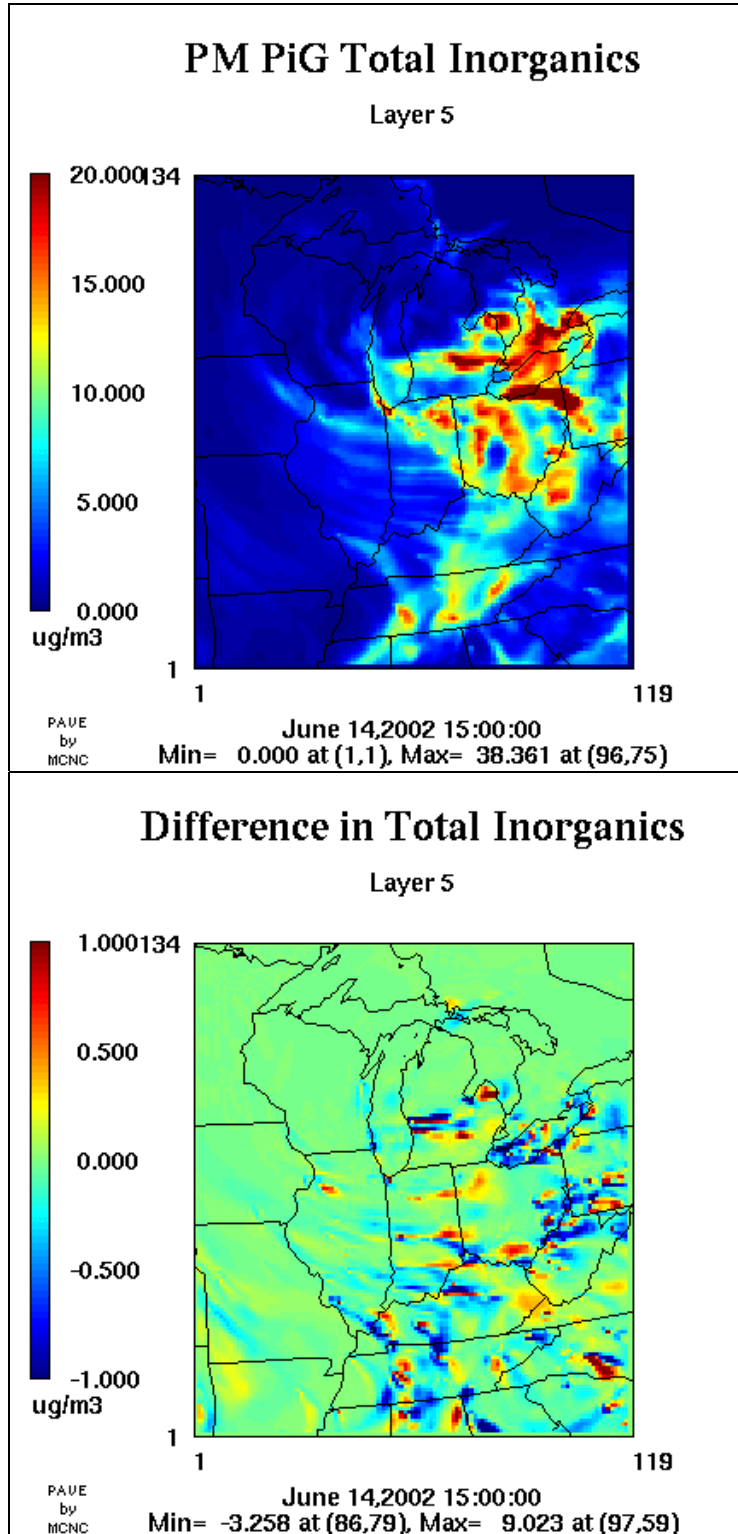


Figure 4-7. Total secondary inorganic PM concentrations ($\mu\text{g}/\text{m}^3$) in layer 5 for the PM PiG run (top) and for the difference between the PM PiG and no-PiG runs (bottom).

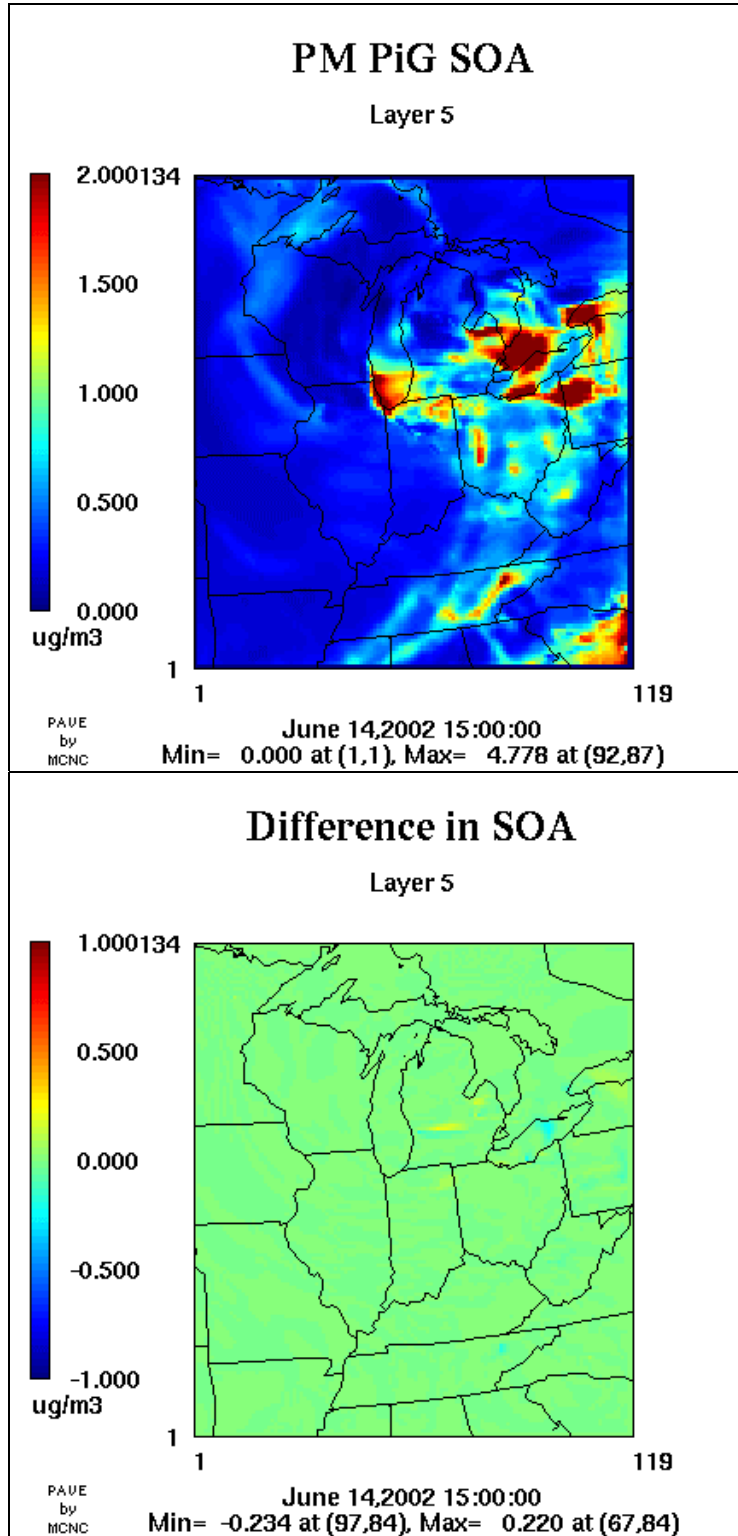


Figure 4-8. Secondary organic aerosol concentrations ($\mu\text{g}/\text{m}^3$) in layer 5 for the PM PiG run (top) and for the difference between the PM PiG and no-PiG runs (bottom).

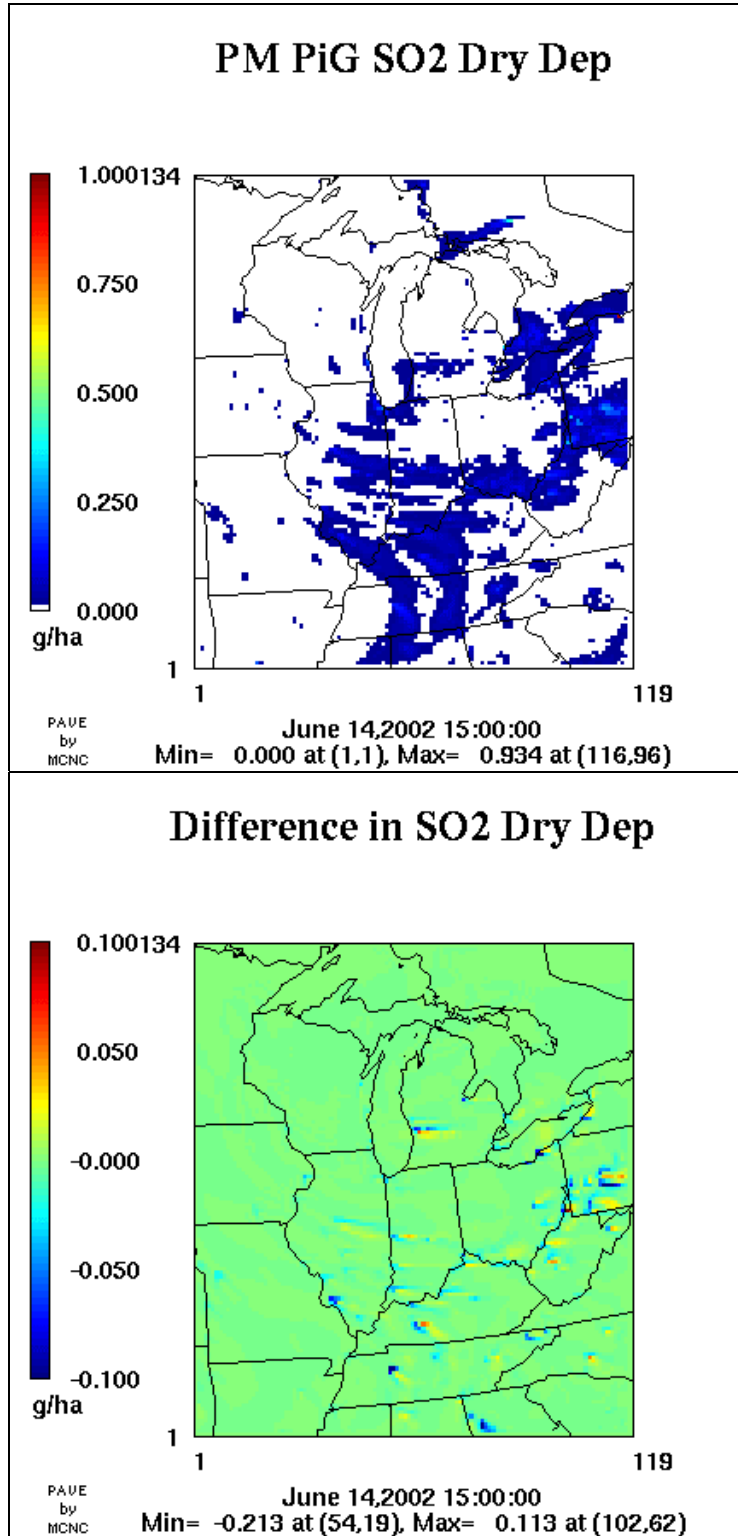


Figure 4-9. SO₂ dry deposited mass (g/ha) for the PM PiG run (top) and for the difference between the PM PiG and no-PiG runs (bottom).

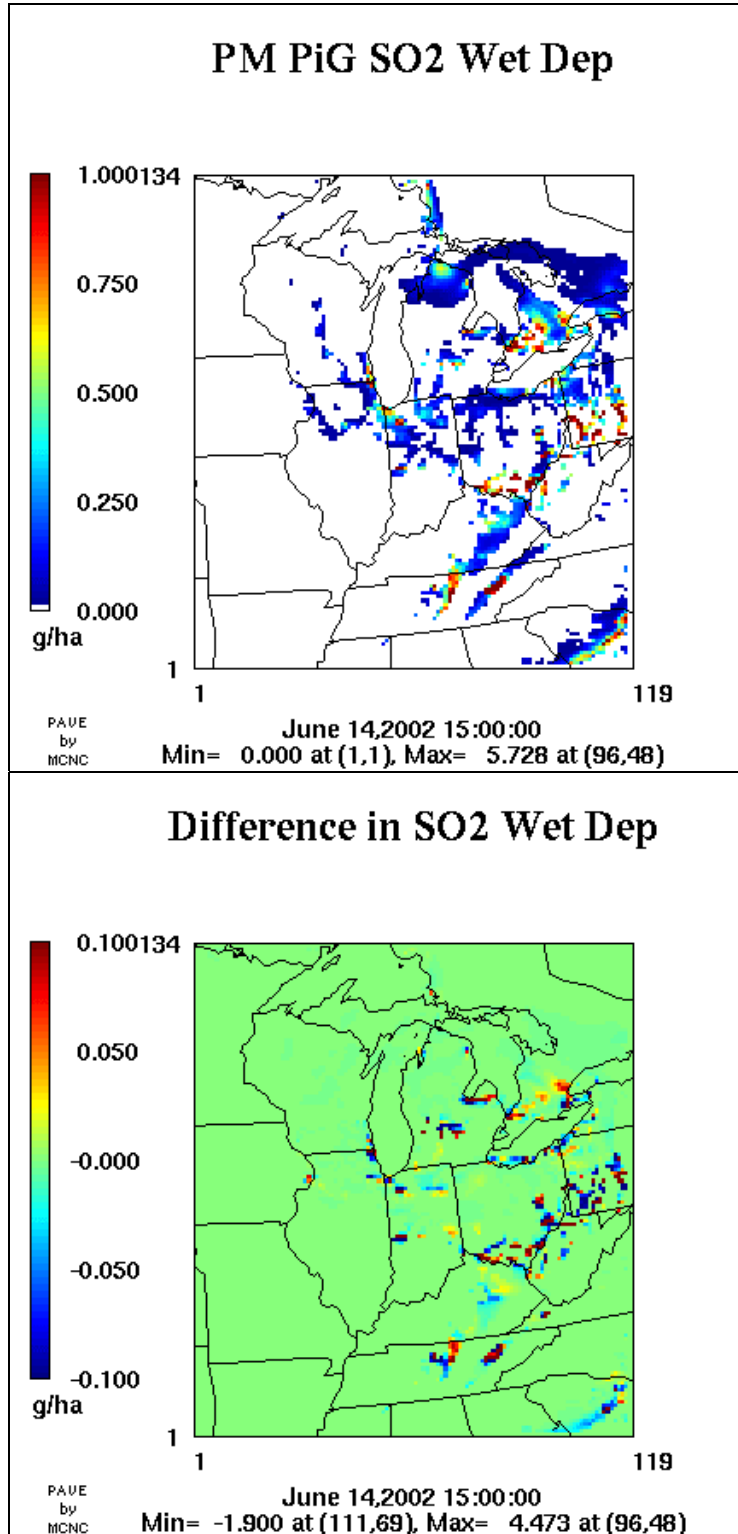


Figure 4-10. SO₂ wet deposited mass (g/ha) for the PM PiG run (top) and for the difference between the PM PiG and no-PiG runs (bottom).

plume impacts are not realized in the average output fields until the PiG mass is actually dumped to the grid. We further suggest that all of the key model species (PM precursors and all PM components) be output to the average files for the full three-dimensional grid. Many of the largest point sources tracked by PiG loft the plumes well above the surface layer, and possibly above the daytime boundary layer in some cases. This will allow some review of the PiG impacts using, for example, the vertical cross section capability of PAVE.

Review of other output files will be just as important. Deposition files can be differenced between no-PiG and PM PiG runs to indicate the plume impacts on deposited mass and rainwater contents. Mass flux summary files should be reviewed for problems in the mass budgets. The most important file in terms of PiG diagnostics is the output diagnostic file (*.diag). For this version of CAMx, additional puff counters and mass summary information have been included in the diagnostic file for review. Additional information can be easily output by re-activating several other write statements within the PiG source code. Key items to watch are described below.

Diagnostic Output Information

At the start of each simulation, whether a cold-start or restart, CAMx echoes the point sources flagged for the PiG treatment. This includes the source identification within the point source file, location coordinates in the current map projection, and stack parameters. Actual emission rates are not printed. In a cold-start, this information is taken directly from the point source file. In a restart, this information is taken from the PiG restart file, and compared to the input point source file to ensure consistency with the previous run. If a mismatch is found in the order or number of PiG sources, the model will stop with an appropriate error message.

At the top of each simulation hour, a series of diagnostic information is printed that summarizes the state of PiG puffs over the previous hour. This includes a summary of the number of puffs killed (mass dumped to the grid) categorized by reason for the termination, the total number of active puffs on each grid at that particular time, and the total PiG and dumped mass summed over the past hour.

The puff kill counters include the following:

- # puffs killed by size :
Reports the number of puffs reaching the maximum size constraint (horizontal area).
- # puffs killed by mass/age :
Reports the number of puffs reaching the minimum remaining mass fraction (<10%) or maximum puff age.
- # puffs killed by bgrd LSODE:
Reports the number of puffs that prohibited LSODE to converge to a solution when operating on the background (grid + overlapping puff) concentrations; this should remain zero for any PiG configuration in which puff overlap is not invoked.

- # puffs killed by tot LSOODE :
Reports the number of puffs that prohibited LSOODE to converge to a solution when operating on the total puff concentration (background + puff increment).
- # puffs killed by bgrd AQPM :
Reports the number of puffs for which background (grid + overlapping puff) concentrations for key inorganic PM precursors and PM components are negative and thus unsolvable by the aqueous and ISORROPIA chemistry routines; this should remain zero for any PiG configuration in which puff overlap is not invoked.
- # puffs killed by total AQPM:
Reports the number of puffs for which total puff concentration (background + puff increment) for key inorganic PM precursors and PM components are negative and thus unsolvable by the aqueous and ISORROPIA chemistry routines.
- # puffs killed by bgrd PM :
Reports the number of puffs for which background (grid + overlapping puff) concentrations for key PM precursors and PM components are negative and thus unsolvable by the aqueous, ISORROPIA, and SOAP chemistry routines; this should remain zero for any PiG configuration in which puff overlap is not invoked.
- # puffs killed by total PM :
Reports the number of puffs for which total puff concentration (background + puff increment) for key PM precursors and PM components are negative and thus unsolvable by the aqueous, ISORROPIA, and SOAP chemistry routines.

We found that it was necessary to kill PiG puffs when chemical conditions either led to a convergence problem in LSOODE (gas-phase chemistry), or when any negative PM precursor/component concentrations were provided to the aqueous/aerosol chemistry routines. When these conditions are met, the puff mass *prior* to the error is dumped to the grid.

It was found in previous testing of IRON PiG for gas-phase photochemistry that, for various well-understood reasons, inconsistencies in chemical evolution between puff mass and grid mass can occasionally drive negative incremental puff concentrations to levels that exceed the positive background concentrations. This results in small negative total concentrations for some species. For gas-phase chemistry, we found that when such negative concentrations are allowed to be passed to LSOODE, the solver effectively runs the reactions associated with negative species backwards, helping to fix (or undo) some of the inconsistency problem by reducing the negative error. In our tests, this has been shown to be effective, but occasionally the problem becomes sufficiently difficult that LSOODE cannot achieve convergence to a solution. When this occurs, the puffs are killed as described above.

This approach cannot work for the PM chemistry modules, however. In those cases, concentrations of specific gas and PM species to be processed by the aqueous, ISORROPIA, and/or SOAP routines must be checked for a negative value prior to calling these modules. When any negatives are found, the puffs are killed as described above.

We find that most puff terminations due to the chemical problems occur within a few hours of cold-starting the model from very clean initial conditions. The reason for this is simple:

chemical processing of fresh point source emissions leads to destruction of certain other species that are available only in the background mass. Various inconsistencies between puff processes and grid processes often lead to larger negative puff increments for such species than the grid mass can support when the background is clean. This problem is exacerbated by puff overlap (thus we recommend not using the puff overlap option). We see a strong drop-off in the number of chemically-driven puff terminations as the day progresses and sufficient grid mass of these secondary species is generated. One way around the cold-start problem might be to introduce the PiG treatment a day or so after the model is initialized to ensure a sufficiently “processed” amount of grid mass. CAMx would need to be revised to handle starting the PiG algorithm during a model restart, as this is currently not possible.

The other important source of information in the hourly PiG diagnostics includes the total PiG and dumped mass summed over the past hour. A typical example is shown below:

```
# active puffs in grid:      1 is 2307
PiG mass:   Total (mol)  Dumped (mol)   Error (mol)   Error (%)
NO          1.378E+06    1.092E+06     0.000E+00    0.000E+00
NO2         9.226E+05    6.737E+05     0.000E+00    0.000E+00
O3         -6.887E+05    -4.857E+05     0.000E+00    0.000E+00
.
.
.
```

This summary is given for each grid, and lists by species the total PiG mass that exists or existed in active PiG puffs within that grid, and the total dumped mass from all puffs within that grid. The error column indicates the extent to which dumped negative mass exceeded the amount of available grid mass in cells receiving the dumps (non-zero errors will only be negative). When negative puffs increments exceed available grid mass, the grid concentrations are set to lower bounds and the difference in mass is added to the error metric. The final column shows the same error but relative (%) to the total amount of dumped mass. In the example above, a large quantity of NO_x is carried by PiG puffs, and they result in a destruction of ambient ozone, which is ultimately dumped to the grid as a relatively large negative impact. The negative ozone increments dumped to the grid were, in all cases, supported by the available grid ozone, resulting in zero errors.

4.4 RECOMMENDATIONS

As suggested above, we recommend that LADCo and the MRPO undertake additional testing and evaluation of the operation and performance of the PM IRON PiG module. Our initial development and preliminary testing of the PM PiG enhancements suggest considering the following:

- Combine co-located source emissions to reduce puff overlap and the number of puffs (this to be handled in pre-processing when PiG sources are selected);
- Improve puff overlap – consider calculating puff overlap integrals, or merging puffs that substantially overlap;
- Consider allowing puffs to grow to twice the grid spacing, rather than the single grid spacing currently employed, to allow smoother transition in plume size representation between plume and grid.

REFERENCES

- ENVIRON. 2004. Design Document: Implementation of PM Chemistry Into the CAMx IRON PiG. Prepared for the Lake Michigan Air Directors Consortium, May 17, 2004.
- EPRI. 2000. SCICHEM Version 1.2: Technical Documentation. Final Report prepared by ARAP/Titan Corporation, Princeton, NJ, for EPRI, Palo Alto, CA. December 2000 (1000713).